Report on the Charissa collaboration's beamtime usage at ANU in 1998

1 Introduction

During 1998 the Collaboration continued to make considerable use of the ANU facility, using time approved by the ANU/EPSRC allocation panel.

On the equipment development side, this year saw the completion of two planned upgrades to the MEGHA array, which were funded in the collaboration's 1996-2000 grant allocation. The first was the installation of the final version of the strip detector mounting ring (replacing a temporary arrangement) which now enables us to mount detectors to pick up light particles over the full angular range of the forward hemisphere. This involved a very complex design and construction process which was carried out with the help of staff from the NPSG at Daresbury and the University of York. The difficult job of providing vacuum feedthroughs for the 320 signals was carried out by the University of Oxford and the new preamps produced by the University of Birmingham. The second upgrade was to the trigger system to provide a fast front-end processing system capable of making more sophisticated trigger decisions than the simple multiplicity threshold system we had been using. This enables much higher rates of potentially interesting events to be written to tape by rejecting "un-interesting" events within a few microseconds and clearing down the readout. This development, using programmable logic arrays, was carried out at the University of Birmingham.

On the physics side, the programme has continued to develop in new directions aligned to our investigations on exotic nuclei at GANIL. The earlier work at ANU on large scale clusters has now come to an end, with a final experiment carried out this year, and has been replaced by investigations in two new directions. There is now an active programme exploring reaction processes leading to highly excited alpha cluster states, backed up by theoretical developments in coupled reactions channels calculations. The coverage of the MEGHA array provides what is probably a unique facility for this - certainly none of our competitors can approach the efficiency which this set-up provides. The second new direction involves studies of the structure of exotic nuclei, as part of a wider programme which also includes experiments using radioactive beams at GANIL. It is our belief that we can use multi-nucleon transfer reactions, using stable beam-target systems, to probe these same structures. Although the cross sections for such reactions are low, our detection systems now have sufficient coverage (almost 4p in the centre of mass) that we can isolate these weak channels and bring all the power of the reaction selectivity to address their structure. Moreover, since these structures are unstable, we can use the techniques of multi-particle decay reconstruction which we have developed to a high art at ANU to determine, accurately, the excitation and spin of the states.

We are particularly interested in an exciting new class of nuclear state which has recently been predicted to exist in light neutron rich nuclei, where cores of alpha particles are bonded together by valence nucleons. The concept of atoms being covalently bonded into molecules by valence electrons, via the exchange interaction, is well established (for example the H2 molecule). Recent studies have suggested that such phenomena may be present on the nuclear scale [1–4]. For example, von Oertzen [3–4] has developed a description of the low lying states of 9Be and 9B in terms of a-n-a and a-p-a molecular structures. In the case of ^{9}Be the additional neutron provides the binding for the unbound ^{8}Be sub-system, much as the covalent bonding of the H^{2+} molecule. Interestingly, the two-centre orbits in which the valence neutron resides, closely resemble those in the atomic molecules, promoting the concept of covalent binding on the nuclear scale, in the form of "molecular analogue" states. These ideas extend to multi-valence particle nuclei such as ^{10}Be, ^{10}B, ^{10}C, ^{11}Be etc., suggestion a rich spectrum of such structures across the sd-shell.

We already have an active programme looking for these structures in the Be, B and C isotopes using the radioactive beams at GANIL. During this year the first two experiments were carried out at ANU and the results of the analysis to date is presented later in this report. We envisage that this programme will develop rapidly over the next few years as an integral part of our work at GANIL and SPIRAL.

The following section of this report provides a brief summary these experiments and equipment development, which were carried out in two periods, Jan/Feb and April, reflecting different modes of operation of the array. Detailed reports on each of the experiments carried out in these two periods are contained in the third and fourth sections of the report.

1.1 Summary of activities

During January and February 1998 the new strip detector array mounting was installed in the MEGHA vacuum chamber and commissioned with a series of experiments. In total 19 days of beamtime were used during this period, including 1 day for the commissioning and installation of the new array and electronics. Following this commissioning, three experiments were carried out. - a measurement of the high spin resonances in ^{12}C+^{12}C which we have identified previously, a pilot study looking at orbiting processes in the ^{12}C+^{28}Si system and an investigation of ^{16}O* $\rightarrow^{12}$C+α breakup. These used a common set-up of eight 16-strip detectors which provided angular coverage from 5° to 60° in the laboratory. Much of the analysis from this period is now completed. To date one paper has been accepted for publication and a number of others are being prepared. Fuller details are provided on each experiment in section 3.

During April 1998 the new trigger system developed to provide a degree of fast front end trigger selection for the MEGHA data acquisition system was installed and commissioned and then used in a series of experiments. In total 14 days of beamtime were used, including 1 day for the commissioning and three experiments were carried out. The first involved an investigation of the out-of-plane angular correlations to determine the reaction mechanism of the ^{12}C(^{24}Mg,^{12}C^{12}C)^{12}C reaction, a measurement in which a mixed mode of heavy ion hybrids and light ion strip detectors was used. This was followed by two measurements in our investigation of the structure of exotic nuclei. The first was a search for the "molecular analogue" states in ^{10}Be and ^{10}C, using two proton and two neutron transfer reactions to populate the nuclei. The second involved an investigation of unbound states in ^{11}Be, as the properties of the states above the neutron separation energy are poorly known and spin/parity assignments are disputed. These higher excited states are important for testing halo models and will yield information about the Borromean ground state of ^{11}Li, which β-decays to ^{11}Be.

2 ANU running Jan/Feb '98

2.1 The Strip detector array

The array [5] consists of a mounting plate which can accommodate either position sensitive strip detectors (PSSD's) or two-dimensional position sensitive detectors (PSD's) in a selection of thirty fixed positions at a typical distance of 150mm from the target.

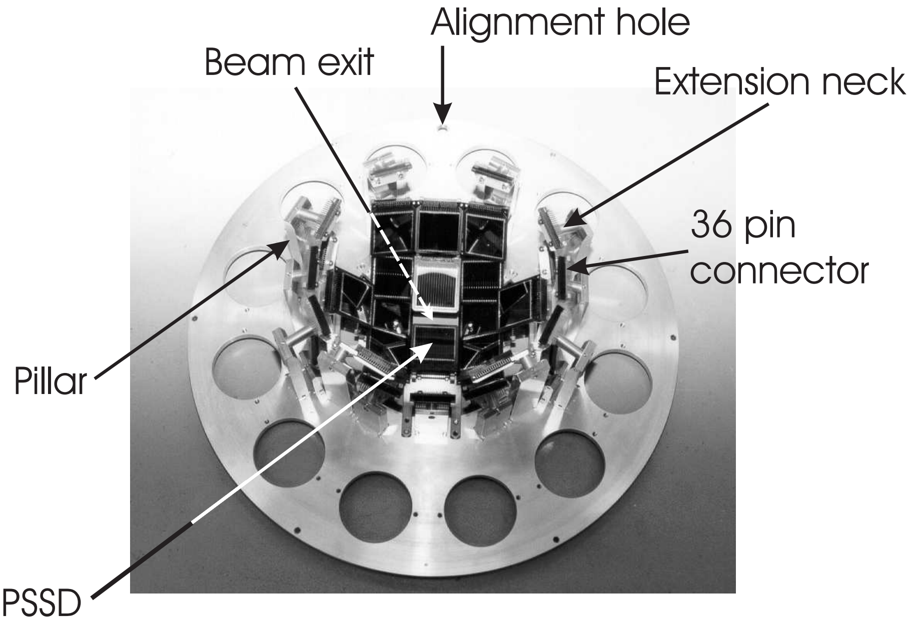

Figure 1: The MEGHA strip detector array mount, partially populated with PSSD's.

With all positions filled the array has almost complete angular coverage from 5° to 85 degrees in the laboratory. At present, the MEGHA data acquisition system provides for up to 320 signal channels. This allows for up to ten PSSD's to be independently instrumented in the array. The mount is designed such that removal of the detectors at forward angles allows PSSD's to be used in conjunction with the MEGHA module Gas-Si-CsI telescopes. Twisted-pair 36way ribbon cables connect the detectors to 42-pin hermetically sealed "Amphenol" connectors fixed in one of the MEGHA chamber

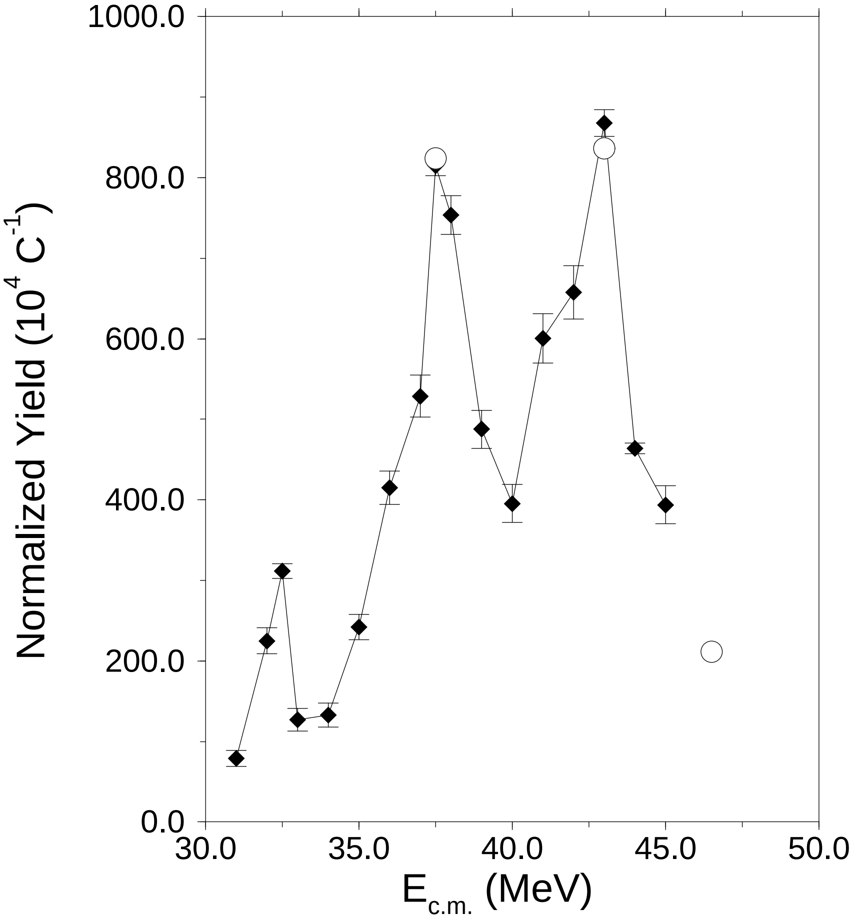

Figure 2: Excitation function for the ^{12}C[^{12}C, ^{12}C(3_1^-)] ^{12}C(3_1^-) reaction (Diamonds from the 4 PSSD measurement of ref. [2]. Open circles from 8 PSSD measurement at ANU)

side flanges. Custom designed preamplifiers are located in racks immediately adjacent to the vacuum vessel.

2.2 High spin resonances in ^{12}C+^{12}C scattering

We have previously observed [6–8] large resonant like structures in the cross section of the 3^-+3^- channel in ^{12}C+^{12}C scattering at $E_{c.m.} = 32.5, 37.5$ and 43 MeV (figure 2). Unfortunately, the angular coverage of the detection system used in the measurements (four position sensitive strip detectors (PSSD's)) was not sufficient to determine the dominant spins of these structures. Following the installation of the new strip detector array, we performed detailed angular correlation measurements at the energies corresponding to the peaks of each resonance. These measurements used 6 days of beamtime. The new strip detector array gave a large efficiency for the detection of high particle multiplicities. This enabled us to use a thin target (10μgcm^{-2}). As a result the resolution obtained in these measurements is significantly improved.

The details of the data analysis and angular correlation method are well described elsewhere [8]. Briefly, the angular correlation for the present case depends on five angles, namely the primary scattering angle ϕ_B^* and the two decay angles χ_B and ψ_B of the ^{8}Be-α relative velocity with respect to the beam for each ^{12}C nucleus. In ref. [8] we demonstrated that the semiclassical angular correlation function for mutual decay could be approximated over the measured angular range by

$$\begin{aligned} W(\phi_B^*, \chi_B, \chi_B', \psi_B, \psi_B') \quad \propto \quad & \frac{1}{\sin\phi_B^*}\left|\sum_{L'} a_{L'} \sin\left[\left(L'+\frac{1}{2}\right)\phi_B^* + k\chi_B + k'\chi_B'\right.\right. \\ & \left.\left. + \frac{\pi}{4}\right]\right|^2 d_{k0}^{I}(\psi_B)^2 d_{k'0}^{I'}(\psi_B')^2 + \frac{A^2}{\sin\phi_B^*} \end{aligned} \qquad (1)$$

where ψ_B,$\psi_B' \simeq \pi/2$. Here $a_{L'}$ is the amplitude for a single value of the partial wave in the final channel L' and A^2 is an incoherent background. The projections of the ^{12}C angular momentum on the z-axis, which is perpendicular to the reaction plane, are k and k'. In ref. [7] we showed that by making assumptions about the quantum numbers k and k' we could define a two-dimensional correlation function $W(\phi_B^*, X)$ where $X = \chi_B \pm \chi_B'$ and hence determine the dominant L' and total angular momentum $J = L' + k + k'$ from the projections of the "ridge" pattern onto a single axis labelled by ϕ_P^*. A slightly different and more rigorous approach is presented in figure 3. In the figure, we compare the projected correlation data with full Monte-Carlo simulations of the reaction for three different consecutive partial waves at each centre of mass energy (figure 3a to 3c). Note that the different partial waves are out of phase away from the centre of the ϕ_P^* range for each energy. In figures 3d to 3f we compare the data with simulations for a coherent sum of two L' values and an incoherent background. The suggested dominant L' values indicated in the figure are consistent with the optimum projection angle θ_P at each energy. We suggest that the dominant L' values for the structures at $E_{c.m.} = 32.5, 37.5$ and 43 MeV are 12, 14 and 16 respectively.

Assuming that these resonances dominate the angular correlations at the

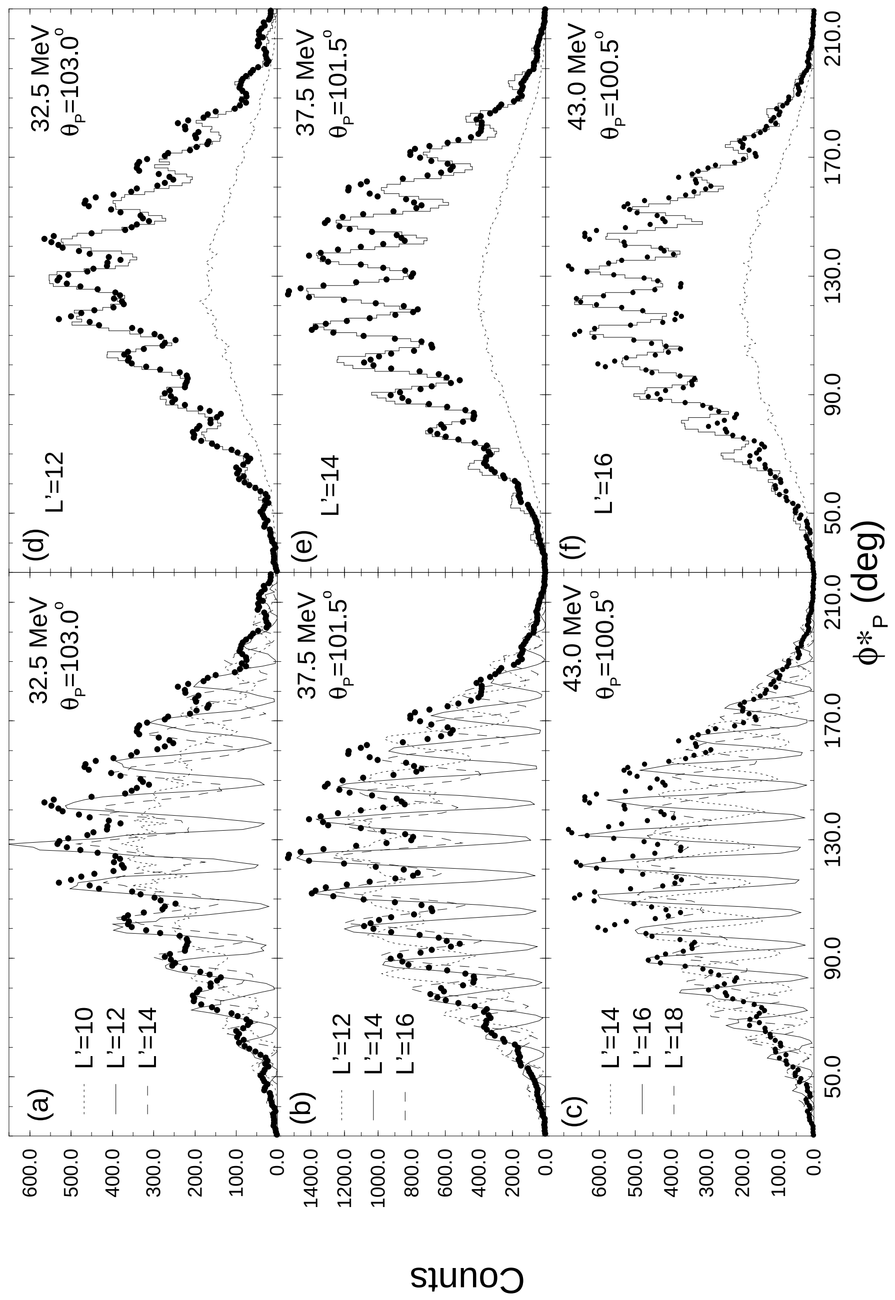

Figure 3: Comparisons of measured and simulated angular correlations projected onto a single axis using the optimum projection angle θ_P indicated at each of the three centre of mass energies. (a–c) Simulation for three consecutive L' values and no incoherent background. (d–f) Simulation including a coherent contribution of two partial waves and an incoherent background. (The background is shown as the dotted curves in the figures scaled by a factor of 0.5 for clarity). (d) $E_{c.m.} = 32.5$ MeV with $a_{12} = 0.92$, $a_{14} = -0.39$ (e) $E_{c.m.} = 37.5$ MeV with $a_{14} = 0.95$, $a_{16} = 0.32$ (f) $E_{c.m.} = 43.0$ MeV with $a_{16} = 0.98$, $a_{18} = -0.22$. The projection angles $\theta_P = 103°, 101.5°$ and $100.5°$ yield $L' = 12.5, 14.2$ and 15.7 respectively which is consistent with our assignments.

centre of each peak in the excitation function they have angular momenta up to $J = L' + 6 = 22$ and are consistent with a rotational band. We believe that these resonances extend the sequence of broad resonances first observed by Cormier *et al.* [9]. A comparison of resonance energies and spins with theoretical calculations support this view [10]. These results have been submitted for publication [10]. We also have results for a number of other channels from this experiment that are being prepared for publication.

2.3 ^{8}Be decay of ^{16}O and ^{12}C

The ^{12}C+^{12}C reaction at $E_{lab} = 93$ MeV was used to study the ^{8}Be decay of highly excited states in ^{16}O and ^{12}C. Approximately 2 days of beamtime were used for these measurements.

The ^{12}C(^{12}C,^{8}Be$_{\rm g.s.}$,^{8}Be$_{\rm g.s.}$)^{8}Be$_{\rm g.s.}$ channel was isolated by detecting 4α particles in the final state and then gating on the ^{8}Be$_{\rm g.s.}$ peak in each $\alpha - \alpha$ relative energy spectrum. Undetected particles were reconstructed from the missing momentum. The parenthood of the three ^{8}Be$_{\rm g.s.}$ nuclei in these events was investigated using a "modified Dalitz plot" [11], as presented in figure 4a. In the geometry of the Dalitz plot, an excited state of the parent nucleus (in this case ^{16}O*) is identified as a stripe at a fixed relative energy E_{ij} between the daughter particles parallel to the sides of the triangle shown. The data are confined to a circle of diameter equal to the available energy in the triple ^{8}Be$_{\rm g.s.}$ final state. The lack of symmetry in the plot is a result of non random particle order in the data sorting routine. Three states in ^{16}O* have been identified (fig. 4b) at $E_x \simeq 19$, 23 and 30 MeV. The spins of the states have been determined using angular correlation techniques. The 6^+ states at 19 and 23 MeV are consistent with those found in previous work [12]. Interestingly, the 8^+ state at 30 MeV is close to the energy predicted for the ^{16}O 4α chain in a coupled-channels cluster model [13]. This model predicts a 10^+ state some 4 MeV higher in energy than the 8^+. Such a state would lie at the edge of the Dalitz plot in figure 4a and is out of the range of the present experiment. We propose to search for the 10^+ state using the technique demonstrated in this measurement [14].

The analysis of ^{12}C(^{12}C,3α)^{12}C$_{\rm g.s.}$ events is slightly more complicated than for the case described above, since the three particles under examination have their energies fixed by the excitation in ^{12}C*, which may take several values. In particular, the decays to ^{8}Be(2^+) are not easily identified due to the large

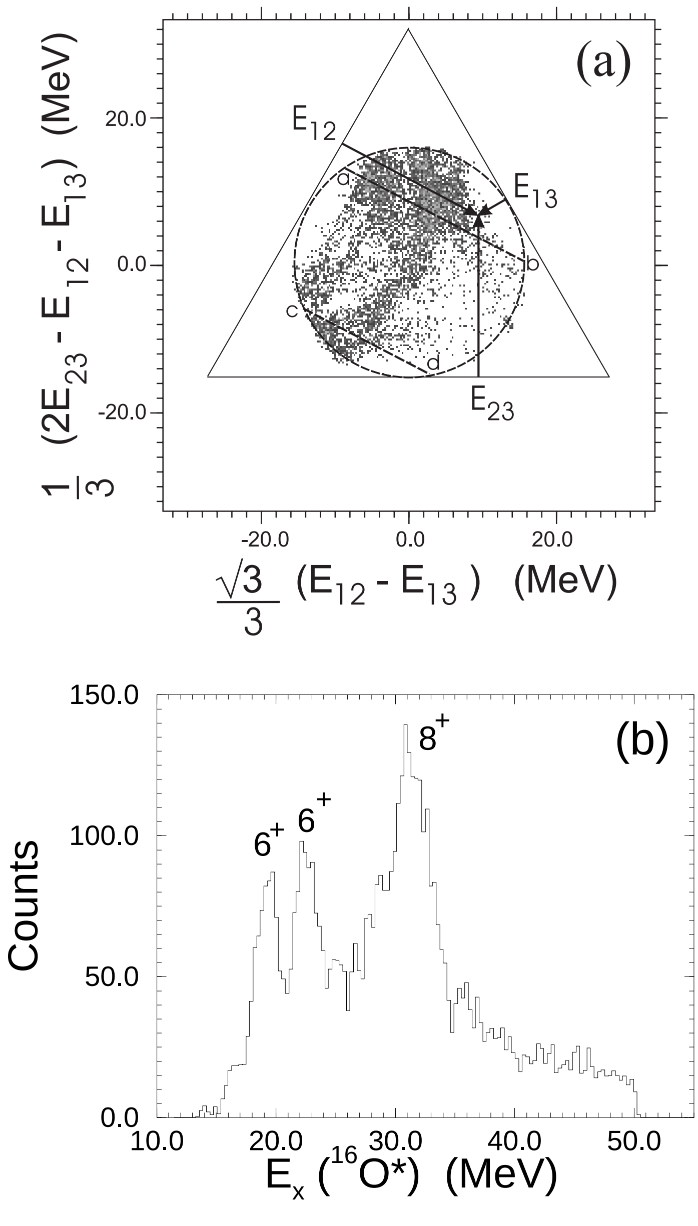

Figure 4: (a) Modified Dalitz plot for the $^8Be_{g.s.}+^8Be_{g.s.}+^8Be_{g.s.}$ final state. (b) Projection of the region abcd (defined in frame a) onto an axis perpendicular to E_{12}.

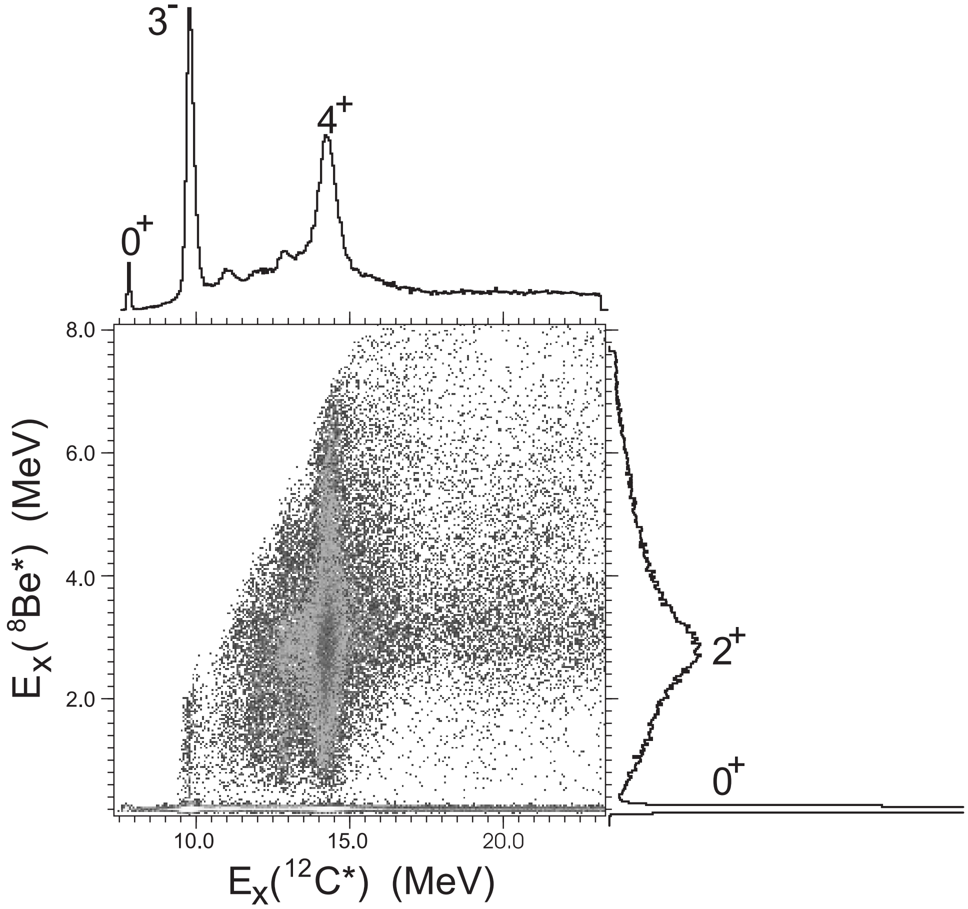

Figure 5: Excitation in ^{12}C* versus excitation in ^{8}Be* for ^{12}C*→ ^{8}Be*+α decays.

width of the state. In order to examine these events the spectrum in figure 5 was constructed. Only one of the three possible $\alpha - \alpha$ relative energies is plotted in this spectrum. If a pair of α particles was found to be consistent with ^{8}Be$_{g.s.}$ decay then that relative energy was plotted, otherwise there was no selection. Hence the ^{8}Be* spectrum contains a background of events where the alpha particle daughters in the sequential decay ^{12}C*→^{8}Be*+α→3α are incorrectly assigned. These data confirm that the 14.08 MeV 4^+ state in ^{12}C decays predominantly via the 2.9 MeV 2^+ state in ^{8}Be [15]. We measure a branching fraction of 0.71±0.01 for this decay.

We propose to investigate the inelastic scattering of ^{12}C+^{12}C to the single and mutual 4_1^+ channels using these analysis techniques [16].

2.4 ^{28}Si+^{12}C orbiting

A pilot study was made into the suitability of the new strip detector array for investigating the phenomenon of dinuclear orbiting [7]. We used approximately 2 days of beamtime to study the ^{28}Si+^{12}C reaction in a kinematic coincidence measurement at $E_{c.m.} = 20.1, 26.0$ and 33.6 MeV. All events in which at least two particles were detected in the strip array were recorded. Following a detailed offline analysis of the data we have discovered that the strip detector array is not well suited to such measurements without more specific event selection. The desired 2-fold elastic and inelastic scattering events in the data were swamped by high fold events. The cross section for scattering to multi-particle final states coupled with the large efficiency for detection of these events in the new array has been found to give an unacceptably large deadtime for the recording of 2-fold coincidences.

2.5 Investigation of ^{16}O$^{*}\rightarrow$ ^{12}C$_{g.s.}$+α breakup

Reactions between an ^{16}O beam and a LiO target (with a natural carbon backing) were used to investigate the energy dependence of the breakup ^{16}O$^{*}\rightarrow$ ^{12}C$_{g.s.}$+α via the single excitation of ^{16}O to the 11.09 MeV 4^+ excited state. Eight days of beamtime were used to measure excitation functions between 26 and 47 MeV in the centre-of-mass. Final state determination and resonant nucleus reconstruction was achieved using a new technique, which relies on a variety of kinematic gates to identify and isolate the breakup channels of interest [21].

Excitation functions for the excitation of ^{16}O* to the 2^+ (9.84 MeV), 4^+ (10.35 MeV) and 4^+ (11.09 MeV) states are given in figure 6. Angular correlation techniques [8] were used to determine the dominant angular momentum associated with specific energies in the centre-of-mass where sufficient data were available (See figure 6). It is interesting to note that the enhancements at 31 MeV and 36 MeV (in the centre-of-mass) in the excitation function for the 11.09 MeV 4^+ excited state are correlated with enhancements observed by Wells *et al* [20] for the single and mutual excitation of ^{16}O to the 3^- (6.13MeV) state. It has been proposed [17] that the ground state of ^{16}O has tetrahedral symmetry. The states usually associated with the ground state rotational band are 0^+ (the ground state), 3^- (6.13 MeV), 4^+ (10.35 MeV), 6^+ (16.29 MeV), 7^- (21.19 MeV) and 8^+ (29.18 MeV). However the

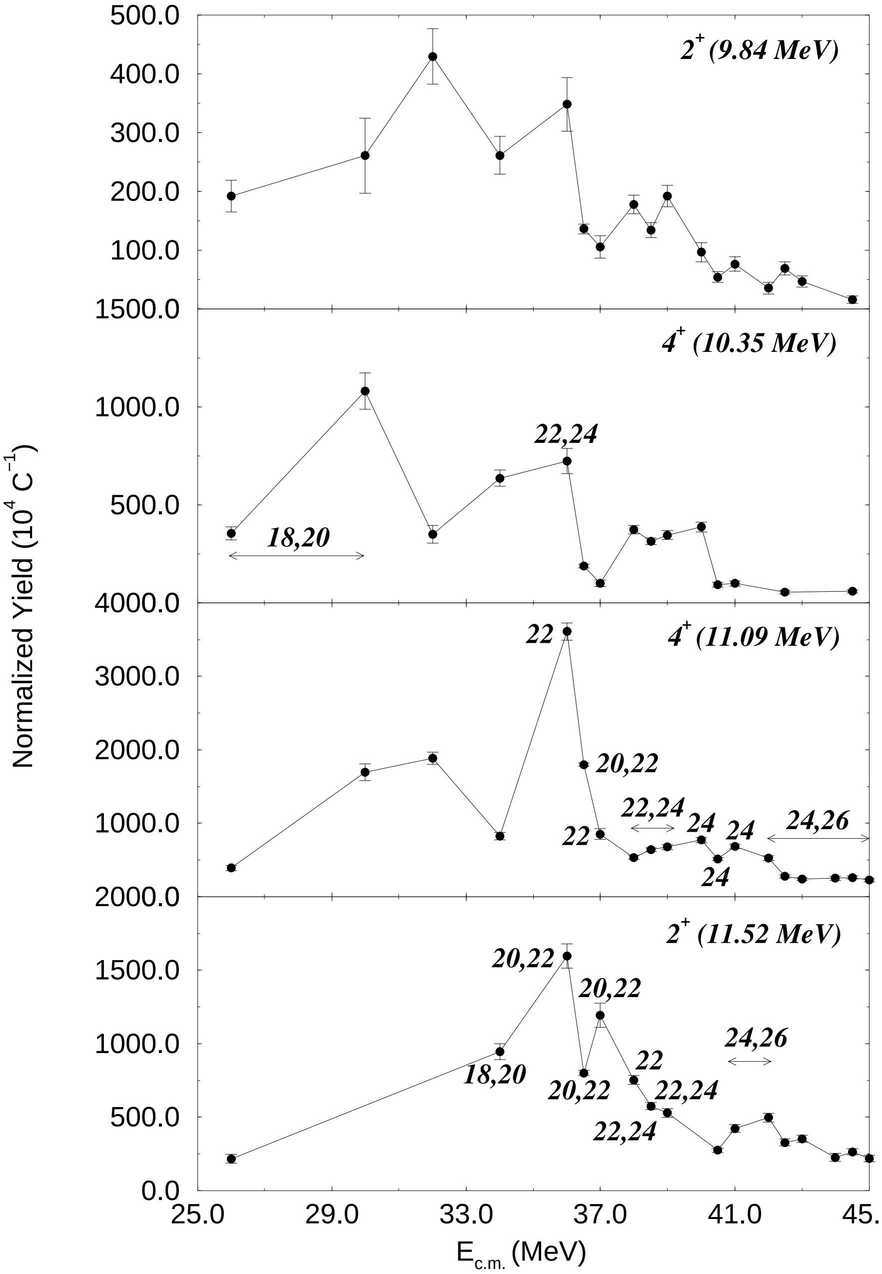

Figure 6: Energy dependence of the ^{16}O(^{16}O,^{16}O$^{*}\rightarrow$ ^{12}C$_{g.s.}$+α)^{16}O$_{g.s.}$ reaction for the ^{16}O* states indicated. Dominant partial waves are given in the figure.

4^+ (10.35 MeV) and 6^+ (16.29 MeV) states also fit into the 4p-4h K=0^+ "kite" rotational band [18]. Better candidates for the tetrahedral band may be the states at 4^+ (11.09 MeV) and 6^+ (14.82 MeV) [19]. If the 4^+ (11.09 MeV) state is a member of the tetrahedral band, it is expected that strong correlations should exist between the excitation function for $^{16}O^* \rightarrow {}^{12}C_{g.s.}+\alpha$ breakup from the 4^+ (11.09 MeV) state, and the measured excitation function for single and mutual excitation to the 3^- (6.13MeV) state. The present results suggest that the 4^+ (11.09 MeV) excited state may indeed be associated with the tetrahedral band in ^{16}O. These results and those on a number of other final state channels are being prepared for publication [21].

3 ANU Running April '98

3.1 The MEGHA Trigger

The MEGHA trigger is a triggering system that attempts to dispense with the need for complex wiring of NIM type modules with vast numbers of cables. In the case of the MEGHA detection system it estimated that approximately 700 cables would be required to complete the typical logic requirements. The alternative approach that is employed uses programmable gate array silicon chips to provide a flexible triggering system which can be changed rapidly without the laborious task of re-cabling. The gate array chips are the Xilinx 4005 which has been packaged in the LeCroy 2366 Universal Logic Module. These CAMAC based devices provide a convenient interface with the 4005 via the CAMAC backplane for programming purposes, and offer 59 configurable input/output channels, per module, accessible via 3, 34 way ECL connectors and 1, 16 way ECL connectors. In addition, the status of two LEDs can be affected under program control. The inputs and outputs from the ULM are ECL convention and are converted to TTL on-board (which also inverts the logical sense of the signals).

The logical condition of the input lines can be tested and additional logic operations performed and the status of the output channels affected accordingly. The internal logic is defined using a suite of Xilinx programs, and then loaded into the ULM via the CAMAC interface. The ".bit" configuration file is loaded from a Personal Computer to the 2366 ULM using a Kinetics Systems Crate Controller and a Kinetics Systems PC Interface card.

The present system contains 6 2366 ULM modules capable of processing 240 channels of information regarding the status of the various detectors in the MEGHA system. The detectors themselves can be configured so that experimental measurements may be made with either 44 detector telescopes composed of three separate detector elements, 10 strip detectors each with 16 strips, or a combination of both strip detectors and telescopes provided the total number of parameters does not exceed the maximum capabilities of the system, i.e. 320 channels. In the former case the trigger is required to processes 132 parameters, and in the case of strip detectors a minimum of 160 channels.

The triggering structure of the MEGHA data acquisition is based on a two level system. The initial trigger is a simple multiplicity condition provided by a collection of 10 LeCroy 4532 MALU units. The 4532 is a multiplicity unit which generates a voltage of 50 mV per active channel. Each of the 10 amplifier crates in the 320 channel system is connected to one MALU unit using ECL type signals. The 10 MALU units are then connected together using the "current carry" feature that permits the discriminators in each of the units to view the total multiplicity in the entire system. Thus the first level trigger is generated from the overall multiplicity of active channels in all the detection elements. The resulting trigger is then used to activate the data acquisition system, which then enters its' event processing mode. The trigger criterion provided by this first level trigger is often not very selective, since it is not possible to restrict the location of the coincident heavy-ions to particular detectors or MEGHA modules. In order to provide a much more selective trigger a second stage in the processing has been used which is the ULM trigger described above. This provides a more discriminating second level trigger in which complex patterns of active detector elements may be demanded. The first level trigger initiates the data processing of the acquisition system and the second level trigger then provides a fast clear if the event is subsequently found to uninteresting, this then opens up the acquisition system to receive further events.

The trigger system was successfully commissioned in March 1998 when it was used for several experimental measurements.

3.2 Unbound states in 11Be

The charge exchange reaction ^{11}B(^{7}Li,^{7}Be)^{11}Be was used to populate excited states in the single neutron halo nucleus, ^{11}Be, above the neutron separation threshold. This experiment was performed at the ANU in April as part of the CHARISSA collaborations program to study halo and halo–related nuclei, complementing radioactive ion–beam experiments performed at GANIL.

The full configuration of the MEGHA array [22] was used for the first time, with the ^{7}Be ejectile identified with isotopic resolution in one of nine Gas–Silicon particle identification telescopes, and the ^{10}Be breakup fragment recorded in one of four 16–strip silicon detectors on the other side of the beam.

The 3–body reaction Q–value can be calculated, by reconstructing the missing momentum of the neutron, after gating on the ^{7}Be ejectile and assuming the detected recoil is ^{10}Be. The Q–value spectrum is shown in Figure 7. The large background contamination (shown as open squares in the figure), is due to mis–identification of either particle, and can be removed by gating out events with an un–physically high neutron energy. The Q–value spectrum shows the excitation of the daughter nucleus, ^{10}Be. The three peaks, from right to left, are for decays to the ^{10}Be ground state, the (2_1^+;3.368MeV) first excited state, and a collection of four states near 6MeV.

The excitation energy of the ^{11}Be nucleus can be calculated using the ^{7}Be energy and angle, or the relative energy of the ^{10}Be and neutron. The former method gives the best resolution. The excitation spectrum for decays to the ^{10}Be ground state is shown in Figure 8, and represents the limit of the data analysis so far. The next step is to measure the relative branching ratio to the 2_1^+ and ground state of ^{10}Be, to give information about the spin and structure of the parent states, and to measure the angular correlations (for decays to the ground state of ^{10}Be) between the two break up fragments to determine the angular momentum of the decay.

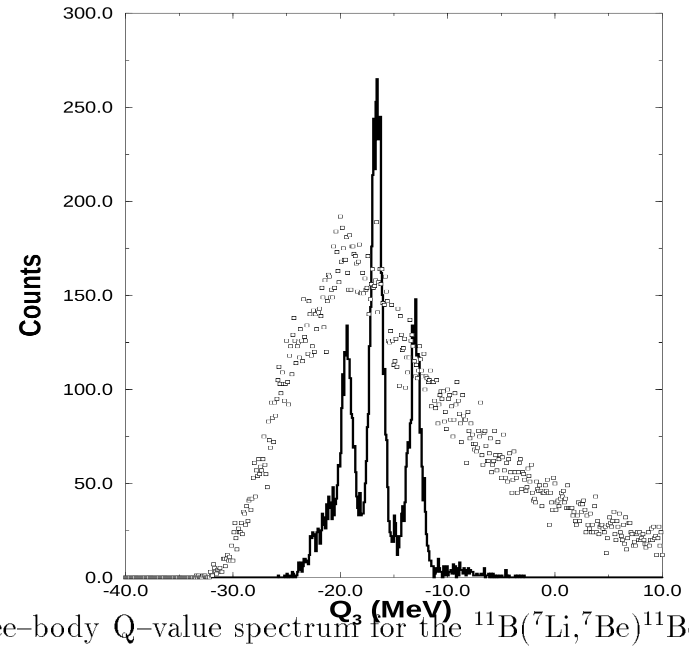

Figure 7: Three–body Q–value spectrum for the ^{11}B(^{7}Li,^{7}Be)^{11}Be→^{10}Be+n reaction. The open squares show the degree of background removal using a neutron energy gate.

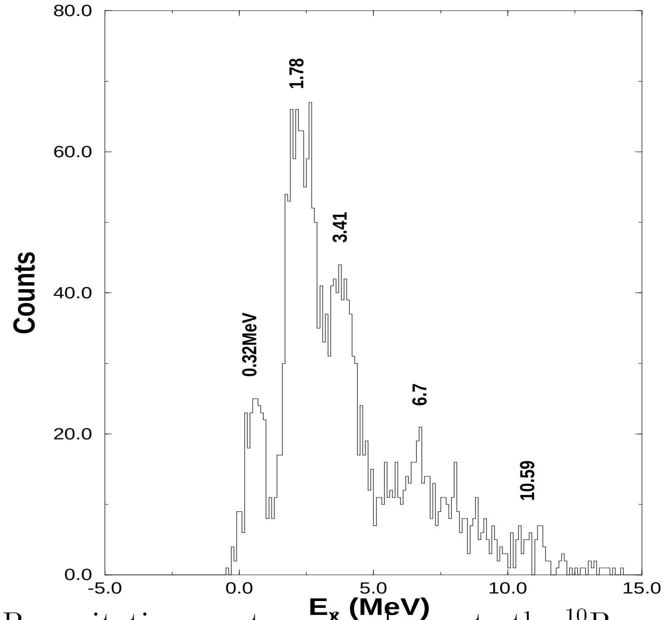

Figure 8: The ^{11}Be excitation spectrum for decays to the ^{10}Be ground state.

3.3 Search for molecular chain states in exotic carbon and beryllium isotopes

The properties of the ^{8}Be nucleus are extremely well described in terms of an alpha-alpha cluster structure. This underlying structure has an important impact upon subsequent protons and neutrons added to the ^{8}Be core as their properties are defined by the two-centre cluster potential.

The resulting valence orbits resemble the orbits of electrons in atomic dimers and hence the term "molecular states". ^{9}Be and ^{9}B are well understood in terms of this picture. The ground state and low lying excited states correspond to highly deformed rotational bands built on nucleons in molecular orbits. The additional nucleon in these systems provides the extra energy required to bind the structure together (the ^{8}Be nucleus is unbound to alpha decay) much as in the case of molecular binding of the H_2^+ molecule by the exchange of an electron.

This picture can be extended to systems with more than one additional nucleon. For example, a series of states at $\sim$6MeV in the nuclei, ^{10}Be and ^{10}B have been described in terms of rotational bands built on configurations of nucleons in two-centre orbits[23]. However in several cases the spectroscopy of these nuclei is uncertain, with spins and parity assignments disputed.

This measurement aimed to study the spectroscopy of these nuclei in an effort to determine their spins and partial decay widths. We utilised the following transfer reactions in order to populate excited states in ^{10}Be and ^{10}C;

$$^{12}\mathrm{C}(^{12}\mathrm{C},^{10}\mathrm{Be})^{14}\mathrm{O}$$
$$^{12}\mathrm{C}(^{12}\mathrm{C},^{10}\mathrm{C})^{14}\mathrm{C}$$

The breakup channels of interest were;

$$\begin{aligned} ^{10}\mathrm{Be} &\rightarrow\ ^{6}\mathrm{Be} +^{4}\mathrm{He},^{9}\mathrm{B} + \mathrm{p}\ \text{and}\ ^{8}\mathrm{Be} + 2\mathrm{p} \\ ^{10}\mathrm{C} &\rightarrow\ ^{6}\mathrm{He} +^{4}\mathrm{He},^{9}\mathrm{Be} + \mathrm{n}\ \text{and}\ ^{8}\mathrm{Be} + 2\mathrm{n} \end{aligned}$$

The measurements were performed at a beam energy of 76MeV with the MEGHA detector's and DA system. The ^{14}O/^{14}C were detected in an array of gas-Si telescope's situated on one side of the beam with ^{10}Be/^{10}C decay products being picked up in a set of four strip detector's on the opposite side.

For channels involving neutron decay all other charged particles were detected and reaction kinematics used to reconstruct the momenta of the unobserved particles.

The key to the measurements was detecting the reactions of interest from a host of other processes leading in certain cases to very similar final states. The MEGHA detection system allows Z determination but does not provide mass resolution making it difficult to identify certain channels in the presence of large backgrounds. Hence, it was necessary to detect all final state particles allowing the reaction Q-value to be determined. By gating around the appropriate area of the spectrum background could then be removed.

After detector calibrations, it was apparent that the reaction channels of interest were unresolvable from other processes. In particular, the reaction $^{12}\mathrm{C}(^{12}\mathrm{C},^{15}\mathrm{O},^{4}\mathrm{He},^{4}\mathrm{He})\mathrm{n}$ looked exactly the same as $^{12}\mathrm{C}(^{12}\mathrm{C},^{10}\mathrm{Be}\rightarrow^{6}\mathrm{He}+^{4}\mathrm{He})^{14}\mathrm{O}$, but the missing neutron energy created a large background over the entire energy range from which the desired channel could not be resolved. Assuming the first reaction and reconstructing E_{tot}, states in ^{15}O are observed (figure 9).

Whilst the initial aims of the experiment have not been realised there is still the possibility of obtaining interesting data. The detector configuration used is sensitive to many other processes, for example work is in progress investigating the structure of ^{7}Be using the reaction ^{12}C(^{12}C,^{17}O)^{3}He,^{4}He. The cross-section and branching ratio of the inverse process ^{3}He(^{4}He,γ)^{7}Be has important implications for the solar neutrino problem [24].

Other possibilities include the investigation of cluster structure in ^{10}B and ^{11}B using the reactions ^{12}C(^{12}C,^{14}N,^{4}He,^{4}He)d and ^{12}C(^{12}C,^{13}N,^{4}He,^{4}He)t respectively. In addition reactions proceeding via the ^{12}C+^{7}Li entrance channel remain to be analysed.

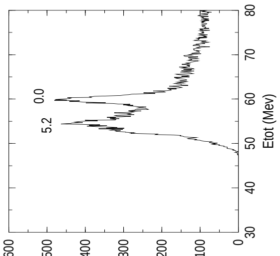

Figure 9: E_{tot} spectrum for ^{12}C(^{12}C,^{15}O,^{4}He,^{4}He)n. The first two excited states in ^{15}O are shown, along with their excitation energy in MeV.

3.4 Investigating the Reaction Mechanism of $^{12}C(^{24}Mg,\ ^{12}C^{12}C)^{12}C$

In the past we have used the $^{12}C(^{24}Mg,\ ^{12}C^{12}C)^{12}C$ breakup reaction to investigate ^{12}C-^{12}C cluster states. However the reaction mechanism by which these states are excited has never been clear. Possible mechanisms include direct excitation, massive (^{12}C) transfer, compound nucleus or resonant processes. Two previous attempts have been made to determine the mechanism by Gyapong et al.[25] and Singer[26]. Unfortunately neither of these experiments gave conclusive results. In March 1998 a further attempt was made to understand this reaction using the large angular coverage of the Multi Element Gas Hybrid Array (MEGHA) to compare the in-plane and out-of-plane breakup cross sections. The experiment was performed using a 150 MeV ^{24}Mg beam and the MEGHA array which allowed us to probe the out-of-plane regions of angular phase space around χ=90 [27]. This has seldom been examined in these breakup reactions since all previous measurements have used detectors arrayed on a reaction plane hence sampling the region around $\chi = 0$.

The aim of this experiment was to compare the experimentally measured ratio of out-of-plane yield to in-plane yield against the same ratio calculated from different reaction models. Theoretical calculations have been performed for coupled channels inelastic scattering, single step inelastic scattering and ^{12}C massive transfer. The results are shown in table 1. The next stage is to calculate the ratio for the statistical compund nucleus and orbiting models.

	Ratio
Experimental	1.26
Coupled Channels	0.90
Single Step	0.75
^{12}C Transfer	1.06

Table 1: Ratio of Out-of-plane yield to In-plane yield

References

[1] Y Kanada-En'yo *et al.*; Phys. Rev. **C52** (1995) 628

[2] Y Kanada-En'yo *et al.*; J. Phys. **G24** (1998) 1499 and references therein

[3] W von Oertzen; Z. Phys. **A354** (1996) 37

[4] W von Oertzen; Z. Phys. **A357** (1997) 355

[5] R.L. Cowin *et al*, to be published in NIMS.

[6] S.P.G. Chappell *et al.*, ANU Annual Report 1995, section C2.3; 1996, section C2.8; 1997,section C.

[7] W.D.M. Rae, S.P.G. Chappell and P.E. Fry, Nuovo Cimento 110A (1997) 1001.

[8] S.P.G. Chappell and W.D.M. Rae, Phys. Rev. C53 (1996) 2879.

[9] T.M. Cormier *et al.*, Phys. Rev. Lett. 40 (1978) 924 and 38 (1977) 940.

[10] S.P.G. Chappell *et al.*, to be published in Phys. Lett. B.

[11] S. Shimoura *et al*, Nucl. Phys. **A452** (1986) 123.

[12] Chevalier, Phys. Rev. C **160** (1967) 827; Brochard, Phys. Rev. C **13** (1976) 967.

[13] A.C. Merchant and W.D.M. Rae, Phys. Rev. C **53** (1996) 775.

[14] S.P.G. Chappell, Charissa proposal CH/PROP/ANU/99/02.

[15] D.D. Caussyn *et al*, Phys. Rev. C **43** (1991) 205.

[16] S.P.G. Chappell, Charissa proposal CH/PROP/ANU/99/01.

[17] J.P. Elliot, J.A. Evans and E.E. Maqueda, Nucl. Phys. **A437** (1985) 208.

[18] R.A. Boldock, B. Buck and J.A. Rubio, Nucl. Phys. **A426** (1984) 222.

[19] D.R. Tilley, H.R. Weller and C.M. Cheves, Nucl. Phys. **A565** (1993) 1.

[20] W.K. Wells, D.P. Bybell and D.P. Balamuth, Phys. Rev. **C25** (1982) 2512.

[21] G.K. Dillon, DPhil. thesis, University of York, U.K. (to be submitted).

[22] R.L. Cowin *et al.*, Nucl. Instr. Meth **A** in press.

[23] W. von Oertzen, Z. Phys. **A 354** (1996) 37.

[24] J.L. Osborne *et al.*, Phys. Rev. Lett. **48** (1982) 1664.

[25] G. Gyapong *et al.*, Nucl. Phys. **A579** (1994) 207

[26] S.M. Singer, Ph.D. Thesis, University of Surrey

[27] C.D. Freeman, ANU Nuclear Physics Annual Report 1997